

ENERGY SUPPLY EFFECT ON SUPERSONIC BOUNDARY LAYER RECEPTIVITY AND STABILITY

Alexander A. Ryzhov* and Vitaly G. Soudakov*

* Central Institute of Aerohydrodynamics, Zhukovsky, Moscow region, 140180, Russia

alex.a.ryzhov@gmail.com; vit_soudakov@tsagi.ru

Keywords: energy supply, receptivity, stability

Abstract

Two-dimensional direct numerical simulation (DNS) of the local heating effect is carried out for near-wall flows over a flat plate at free-stream Mach number 6. The influence of energy source parameters to receptivity and stability is studied.

1 Introduction

Laminar-turbulent transition prediction is important for aerothermal design of high-speed vehicles [1]. The first reason is that early transition leads to the increase of drag and hence the loss of the aircraft efficiency. The second one is associated with wall heat fluxes growth. This motivates extensive experimental, theoretical and numerical studies of transition at supersonic and hypersonic speeds. Progress made in the transition prediction methodology for high speeds is reviewed in [2]. Both surface roughness and external disturbances could result in the transition. For the case of external disturbances, there are at least two routes leading to turbulence in the boundary-layer flow. The first route occurs in “quiet” free stream conditions on aerodynamically smooth surfaces. It involves receptivity, linear phase and nonlinear breakdown to turbulence. Receptivity refers to the mechanism by which free-stream disturbances enter the boundary layer and generate unstable modes. The linear phase is associated with the downstream evolution of these modes and is described by the linear stability theory (LST) [3]. The nonlinear breakdown occurs when the disturbance amplitudes achieve a certain critical level. The second route of transition is observed in “noisy”

environments and involves bypassing of the linear phase.

The receptivity to acoustic disturbances was intensively studied theoretically [4], experimentally [5] and numerically [6]. The receptivity to free-stream entropy and vortical disturbances was investigated worse. DNS of the receptivity of a flat-plate boundary layer to entropy and vorticity free-stream waves with several positive angles of inclination was investigated in [7]. Fedorov and Tumin [8] analyzed an initial value problem for a two-dimensional wavepacket induced by a local two-dimensional disturbance in a hypersonic boundary layer. Characteristics of the wavepacket generated by an initial temperature spot were numerically calculated. It was shown that the hypersonic boundary layer is receptive to vorticity/entropy disturbances in the region of synchronization between entropy/vorticity modes of temporal continuous spectrum and discrete spectrum modes.

Schneider et al. [9-11] experimentally investigated disturbances induced by a laser beam on a cone at hypersonic flow conditions. It was shown that these disturbances have approximately Gaussian radial temperature distributions. The heat spot generates both acoustic and vorticity disturbances while transmitting through the shock. Zhong et. al. [12] carried out DNS of a single entropy spot propagating past a sharp cone for the conditions of Boeing/AFOSR Mach-6 Quiet tunnel in Purdue University [13].

Heitmann et al. performed experimental and numerical simulation of Mach 6 boundary layer response to laser generated disturbances [14, 15]. The model was 7° half angle sharp cone. It was shown that a second mode evolves due to

the interaction of a laser induced shock wave with the boundary layer. The simulated wave exhibits similar properties like naturally occurring waves, e.g. concerning their frequency and amplification.

Two-dimensional DNS of a flat-plate boundary layer receptivity to free-stream temperature spottiness in Mach-6 free stream was carried out in [16]. The DNS results were compared with the theoretical predictions.

Along with receptivity studies permanent energy supply is also treated as a tool for stability control. Stability of subsonic compressible laminar boundary layer with volume energy supply was studied in [17]. It was shown that volume energy supply can lead to flow stabilization and reduced perturbation growth rates.

In the first part of the present paper, DNS of the receptivity of a flat-plate boundary layer to energy source-induced disturbances is carried out.

In the second part of the paper, two-dimensional DNS of a flat-plate boundary layer stability in the presence of a local volume heat supply in Mach-6 free stream is carried out. Heat supply changes the mean flow. As a result, the maximum amplitude of the disturbances decreases. Various longitudinal locations of the heat source are considered.

2 Problem formulation and numerical method

Viscous two-dimensional unsteady compressible flows are governed by the Navier-Stokes equations resulted from the conservation laws of mass, momentum and energy. Numerical simulations are carried out for a flat plate with a sharp leading edge.

The flow variables are made nondimensional using the steady-state free-stream parameters (denoted by subscript “ ∞ ”): $(u, v) = (u^*, v^*) / U_\infty^*$ are longitudinal and vertical velocity components, $p = p^* / (\rho_\infty^* U_\infty^{*2})$ is pressure, $\rho = \rho^* / \rho_\infty^*$ is density, $T = T^* / T_\infty^*$ is temperature. The nondimensional coordinates

are $(x, y) = (x^*, y^*) / L^*$, and time is $t = t^* U_\infty^* / L^*$, where U_∞^* is the free-stream velocity, L^* is the plate length. Hereinafter, asterisks denote dimensional variables. The fluid is supposed to be a perfect gas with the specific heat ratio $\gamma = 1.4$ and Prandtl number $Pr = 0.72$. Calculations are performed for Mach number 6 and Reynolds number (based on free-stream parameters and plate length) $Re_L = \rho_\infty^* U_\infty^* L^* / \mu_\infty^* = 2 \times 10^6$, where μ_∞^* is free-stream dynamic viscosity coefficient. The viscosity-temperature dependence is approximated by the power law $\mu^* / \mu_\infty^* = (T^* / T_\infty^*)^{0.7}$. The second viscosity is assumed to be zero. The plate has a nominally sharp leading edge; i.e. the leading-edge radius is so small that the bluntness-induced entropy layer does not affect receptivity and stability of the boundary layer.

The boundary conditions on the plate surface are: the no-slip condition $(u, v) = 0$, the adiabatic wall condition $\partial T_w / \partial n = 0$ for the steady state solution. On the outflow boundary, the unknown dependent variables are extrapolated using the linear approximation. On the inflow and upper boundaries, conditions correspond to the free stream. Details of the problem formulation and governing equations are discussed in [18].

The problem is solved numerically using the implicit second-order finite-volume method described in [18]. The advection terms are approximated by the third-order WENO scheme to decrease the numerical dissipation. The computational grid has 2001×301 nodes, so that there are at least 45 grid nodes per the disturbance wavelength and approximately 400 time steps are per the disturbance period. The grid is clustered in the direction normal to the plate surface so that the boundary-layer region contains approximately 50% of nodes.

3 Receptivity to small energy disturbances

At first, a steady-state solution is calculated to provide the mean flow without energy source.

The steady pressure field shown in Fig. 1 indicates that the viscous-inviscid interaction between the boundary layer and the free stream leads to a shock wave emanating from the plate leading edge.

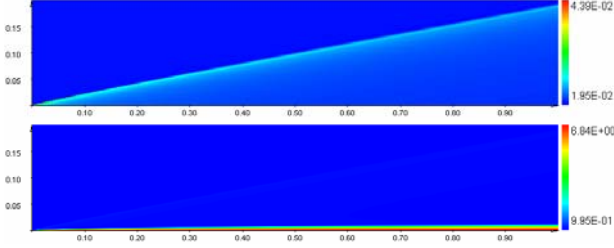


Fig. 1. The mean-flow pressure and temperature fields over a flat plate.

Then energy source (source term of energy equation)

$$E'(x, y; t) = \varepsilon \exp \left[\frac{-(x - x_0)^2 - (y - y_0)^2}{\sigma_0^2} \right] \times \\ \times \delta(\omega t - 2\pi n), n \in \mathbb{Z}, \\ \delta(\omega t - 2\pi n) = \begin{cases} 1, \omega t = 2\pi n \\ 0, \omega t \neq 2\pi n \end{cases}$$

is induced into the boundary layer and unsteady problem is solved. Here ε is intensity of energy source, (x_0, y_0) is center of induced disturbance, σ_0 is characteristic radius, $\omega = \omega^* L^* / V_\infty^*$ is circular frequency.

The energy disturbance has amplitude $\varepsilon = 0.1$ at which the receptivity process is linear. The disturbance of temperature field corresponds to $\varepsilon_T = 0.0095$. The disturbance frequency $\omega = 260$ corresponds to the frequency parameter $F = \omega / \text{Re} = 1.3 \times 10^{-4}$ at which the Mack second mode is unstable for $x > 0.7$. The temperature disturbance is zero on the plate surface, $T'_w = 0$. Disturbance width is $\sigma_0 = 0.5\delta_e$. Hereafter $\delta_e = 0.008$ is the boundary layer thickness at $x = 0.5$. Longitudinal location is $x_0 = 0.3$ which is downstream of the bow shock. The different initial vertical locations $y_0 = (0.5\delta_e, 0.75\delta_e, \delta_e, 1.25\delta_e, 1.5\delta_e)$ of spots are considered. In each case, the calculations are

carried out until a quasi-periodic regime is established.

Small energy source induces acoustic and entropy disturbances penetrating the boundary layer and exciting unstable modes. Pressure disturbances at fixed moment in time (difference between instant pressure and mean flow pressure) along the plate surface are presented in Fig. 2. It is shown that induced energy spots generate unstable disturbances in the boundary layer which can lead to laminar-turbulent transition.

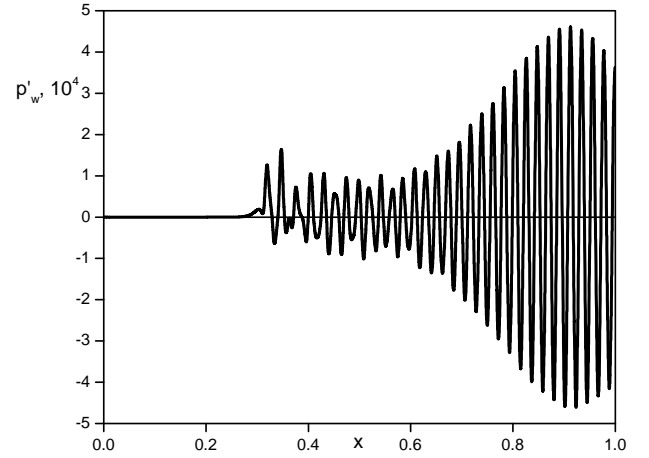


Fig. 2. Pressure disturbances on the plate at $y_0 = 1.125\delta_e$.

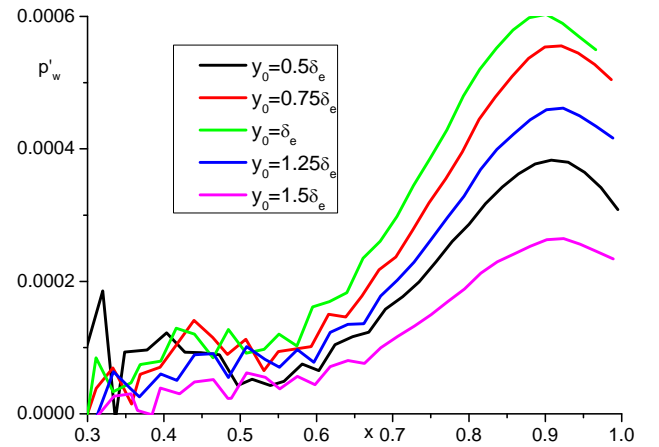


Fig. 3. Wall pressure disturbances envelopes for different vertical positions y_0 .

Wall pressure disturbance envelopes are shown in Fig. 3 for different vertical position y_0 . Maximal pressure disturbances are reached in the case $y_0 = \delta_e$. The dependence of receptivity coefficient $T'_{\max} / \varepsilon_T$ from the vertical source position above the plate y_0 is presented in Fig. 4. Here ε_T -temperature disturbance

amplitude at heat source center, T'_{\max} - temperature disturbances maximum inside the boundary layer. Receptivity coefficient also reaches maximum at $y_0 \approx \delta_e$.

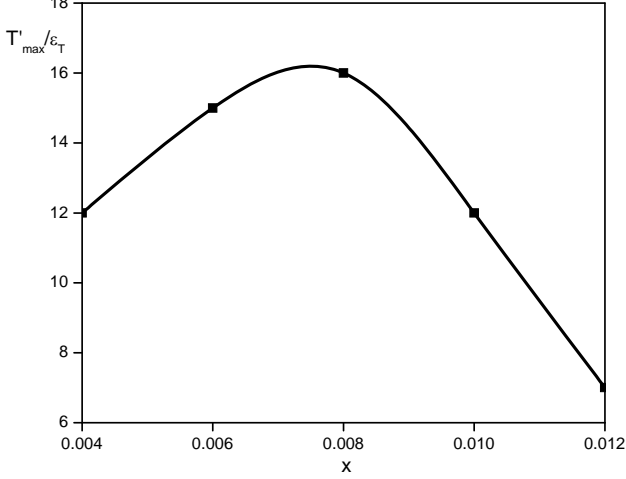


Fig. 4. Receptivity ϵ_T coefficient as a function of vertical source position y_0 .

4 Stability of the boundary layer with energy supply

In this section, two-dimensional DNS of flat-plate boundary layer stability in the presence of a permanent local volume heat supply in Mach-6 free stream is carried out. Heat supply changes the mean flow. As a result, the maximum amplitude of the disturbances can decrease. Various longitudinal locations of the heat source are considered.

The heat supply is simulated by energy source $E_0(x, y)$ added to the Navier-Stokes equations in the form

$$E_0(x, y) = A \exp \left[-\frac{(x - x_0)^2 + (y - y_0)^2}{\sigma_0^2} \right]$$

where $A = 0.01$ is the heat source amplitude, x_0 varying from 0.1 to 0.9, $y_0 = \delta_e = 0.008$, $\sigma_0 = 0.004$. The heat source is placed near the upper edge of the boundary layer.

The mean flow pressure and temperature fields near the flat plate with heat source ($x_0 = 0.5$) are shown in Fig. 5. Heat source leads to local increase of the boundary layer thickness and formation of the shock wave. Wall pressure and temperature for different

positions of heat supply are presented in Fig. 6 and 7 respectively.

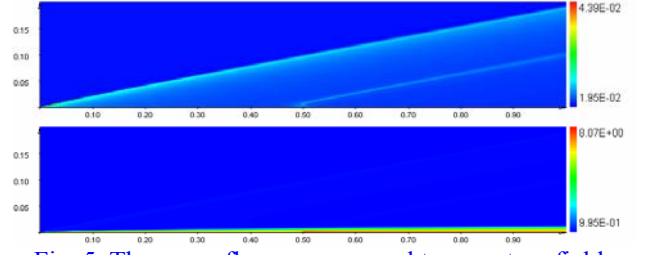


Fig. 5. The mean-flow pressure and temperature fields over a flat plate, $x_0 = 0.5$.

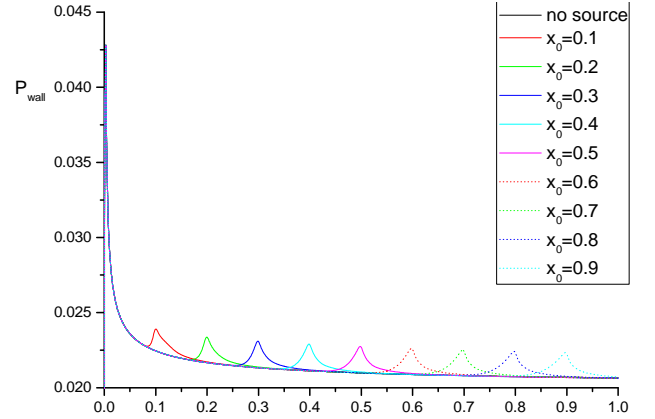


Fig. 6. Wall pressure for various x_0 .

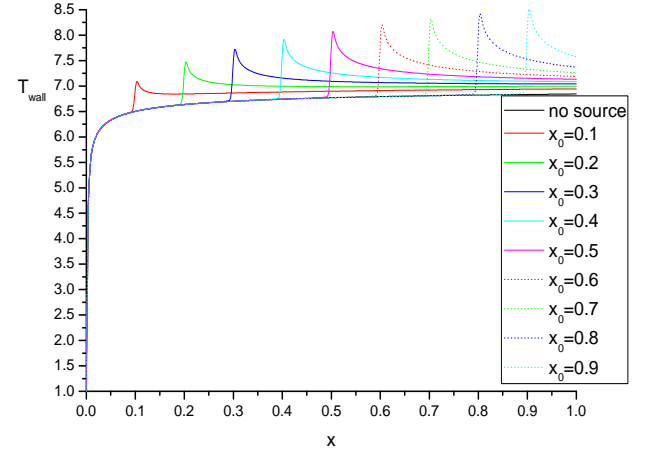


Fig. 7. Wall temperature for various x_0 .

To investigate the boundary-layer instability initial disturbances are induced by a local periodic suction-blowing in the leading-edge vicinity [18]. The mass flow on the plate surface is given by

$$q_w(x, t) = \frac{\rho_w^* v_w^*}{\rho_\infty^* U_\infty^*} = \epsilon \sin \left(2\pi \frac{x - x_1}{x_2 - x_1} \right) \sin(\omega t),$$

$$x_1 \leq x \leq x_2, \quad t > 0$$

where ε is forcing amplitude; $x_1 = 0.0358$, $x_2 = 0.0495$ are boundaries of the local suction-blowing region; the circular frequency $\omega = 260$ corresponds to high-frequency disturbances including unstable second-mode waves. The amplitude $\varepsilon = 6 \times 10^{-4}$ was chosen small enough to ensure validity of the linear approximation. In the unsteady problem, the wall temperature corresponds to adiabatic wall, $T_w(x, t) = T_{ad}(x)$; i.e., the temperature disturbances on the wall are zero.

Local blowing-suction excites unstable disturbances in the boundary layer reaching its maximum at $x \sim 0.9$. Heat supply changes locally the boundary layer properties leading to change of its stability characteristics. It results in the loss of maximum amplitude of disturbances inside the boundary layer.

Wall pressure disturbances for the case of heat supply at $x_0 = 0.5$ and $x_0 = 0.9$ are shown in Fig. 8 and 9 respectively. There is a sharp decrease of disturbances in the case of $x_0 = 0.9$. Comparison of envelopes of wall pressure disturbances is presented in Fig. 10 for different positions of heat supply. Black curve corresponds to the case without heat supply. Pressure and temperature disturbance fields ($0.7 \leq x \leq 1$) are shown in Fig. 11 and 12 for the case without heat supply and with heat supply at $x_0 = 0.9$.

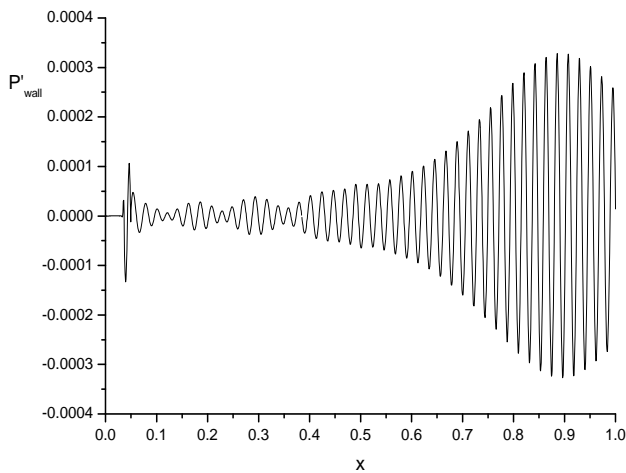


Fig. 8. Wall pressure disturbances, $x_0=0.5$.

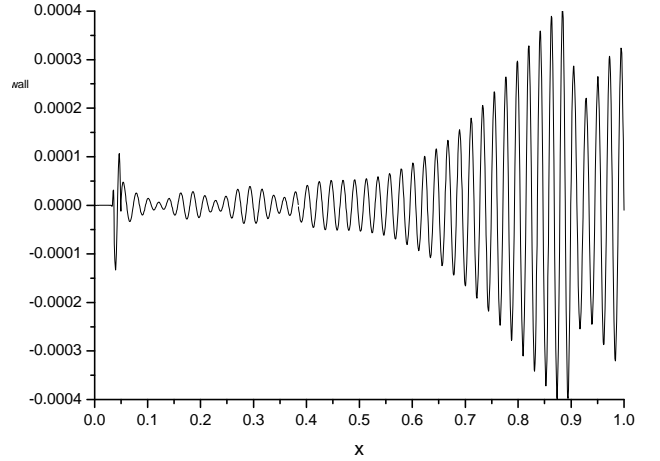


Fig. 9. Wall pressure disturbances, $x_0=0.9$.

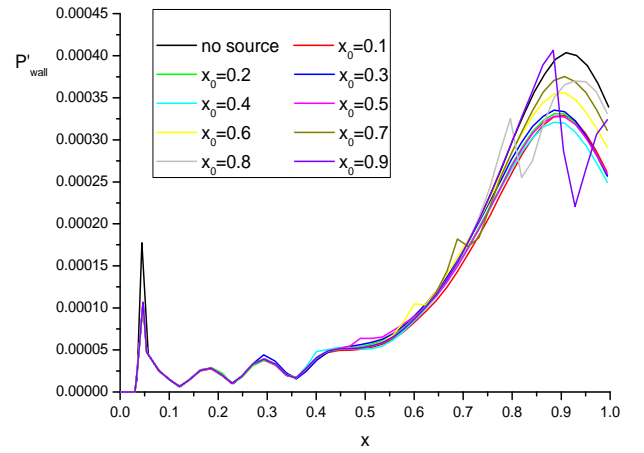


Fig. 10. Envelopes of pressure disturbances on the wall for various x_0 .

The results of unsteady numerical simulations show that local heat supply can lead to the decrease of unstable modes amplitude. The strongest effect is achieved for $x_0 < 0.5$. Amplitude of unstable disturbances decreases up to 20%.

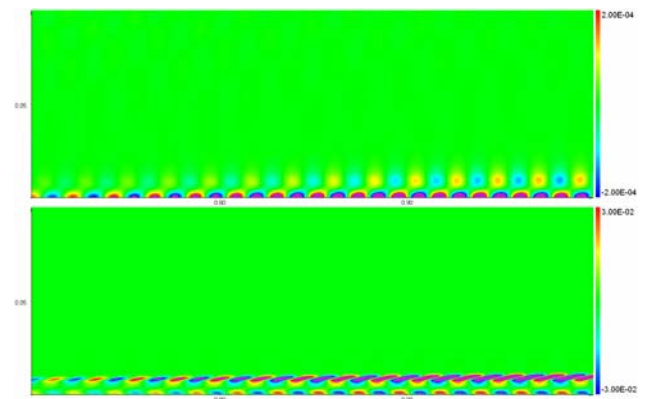


Fig. 11. Pressure and temperature disturbances without heat supply.

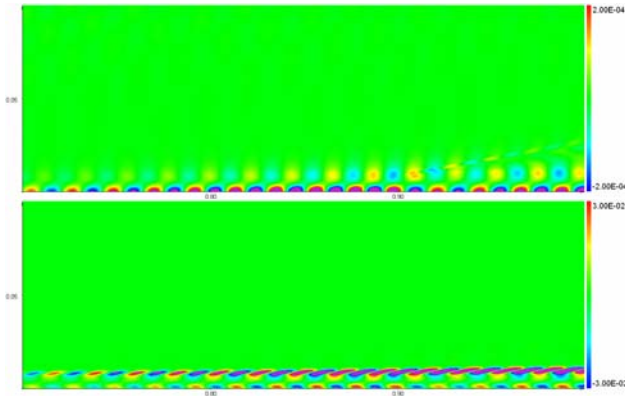


Fig. 12. Pressure and temperature disturbances with heat supply at $x_0=0.9$.

Note, that disturbances at a given frequency reaches its maximum at $x=0.9$ and this position is independent from the heat supply location.

4 Summary

Two-dimensional direct numerical simulation of receptivity of a flat-plate boundary layer to the disturbances induced by local periodic energy source in the boundary layer is carried out. Different vertical positions of the source are considered. Disturbances and receptivity coefficient reach maximum when energy source is induced near the upper edge of the boundary layer.

Two-dimensional DNS of a flat-plate boundary layer stability in the presence of a local permanent volume heat supply in Mach-6 free stream is carried out. Heat supply changes the mean flow. As a result, the maximum amplitude of the disturbances can decrease. Various longitudinal locations of the heat source are considered.

Local heating effectively diminishes growth rate of unstable disturbances. Particularly the second-mode amplitude decreases up to 20% on the surface with local heating source placed at $x<0.5$.

Acknowledgments

This work was supported by the Russian government under grant “Measures to Attract Leading Scientists to Russian Educational Institutions” (contract No. 11.G34.31.0072).

References

- [1] Reed H.L., Kimmel R., Schneider S. and Arnal D. Drag prediction and transition in hypersonic flow. *AIAA Paper* 97-1818, 1997.
- [2] Malik M., Zang T., and Bushnell D. Boundary layer transition in hypersonic flows. *AIAA Paper* 90-5232, 1990.
- [3] Mack L. M. Boundary layer linear stability theory, special course on stability and transition of laminar flow. *AGARD Rept.* Vol. 709, pp. 379-409, 1984.
- [4] Fedorov A.V. Receptivity of a high-speed boundary layer to acoustic disturbances. *J. Fluid Mech.*, Vol. 491, pp. 101-129, 2003.
- [5] Maslov A.A., Shiplyuk A.N., Sidorenko A., Arnal D. Leading-edge receptivity of a hypersonic boundary layer on a flat plate. *J. Fluid Mech.* Vol. 426, pp. 73-94, 2001.
- [6] Soudakov V.G. Numerical simulation of the effect of acoustic wave inclination angle on a hypersonic boundary-layer receptivity. *TsAGI Science Journal.* Vol. 41(3), pp. 269-284, 2010.
- [7] Ma Y., Zhong X. Receptivity of a supersonic boundary layer over a flat plate. Part 3. Effects of different types of free-stream disturbances. *J. Fluid. Mech.* Vol. 532, pp. 63-109, 2005.
- [8] Fedorov A.V. and Tumin A.M. Initial-value problem for hypersonic boundary-layer flows. *AIAA J.*, Vol. 41, No 3, pp. 379-389, 2003.
- [9] Schneider S.P., Collicott S.H. and Schmeisseur J.D. Laser-generated localized freestream perturbations in supersonic and hypersonic flows. *AIAA J.*, Vol. 38, No.4, pp. 666-671, 2000.
- [10] Schmeisseur J.D., Schneider S.P. and Collicott S.H. Supersonic boundary-layer response to optically generated freestream disturbances. *Experiments in Fluids*, Vol. 33, pp. 225-232, 2002.
- [11] Salyer T.R., Collicott S.H. and Schneider S.P. Characterizing laser-generated hot spots for receptivity studies. *AIAA J.*, Vol. 44, No 12, pp. 2871-2878, 2006.
- [12] Huang Y. and Zhong X. Numerical study of laser-spot effects on boundary-layer receptivity for blunt compression-cones in mach-6 freestream. *AIAA Paper* 2010-4447, 2010.
- [13] Schneider S.P., Wheaton B.M., Julinao T.J., Berridge D.C., Chou A., Gilbert P.L., Casper K.M. and Steen L.E. Instability and transition measurements in the mach-6 quiet tunnel. *AIAA Paper* 2009-3559, 2009.
- [14] Heitmann D., Radespiel R., Knauss H. Experimental study of mach 6 boundary layer response to laser generated disturbances. *AIAA Paper* 2011-3876, 2011.
- [15] Heitmann D., Radespiel R. Simulation of the interaction of a laser generated shock wave with a hypersonic conical boundary layer. *AIAA Paper* 2010-3875, 2010.
- [16] Fedorov A.V., Ryzhov A.A., Soudakov V.G. Numerical and theoretical modeling of supersonic

boundary-layer receptivity to temperature spottiness.
AIAA Paper 2011-3077, 2011.

- [17] Kazakov A.V., Kogan M.N. Stability of subsonic laminar boundary layer on a flat plate with volume energy supply. *Fluid Dynamics*, № 2, pp. 62-67, 1988.
- [18] Egorov I.V., Fedorov A.V. and Soudakov V.G. Direct numerical simulation of disturbances generated by periodic suction-blowing in a hypersonic boundary layer. *Theoret. Comput. Fluid Dynamics*, Vol. 20, No. 1, pp. 41-54, 2006.

Copyright Statement

The authors confirm that they, and/or their company or organization, hold copyright on all of the original material included in this paper. The authors also confirm that they have obtained permission, from the copyright holder of any third party material included in this paper, to publish it as part of their paper. The authors confirm that they give permission, or have obtained permission from the copyright holder of this paper, for the publication and distribution of this paper as part of the ICAS2012 proceedings or as individual off-prints from the proceedings.